Analytical Estimation of Radar Cross Section of Arbitrary Compact Dipole Array

H. L. Sneha, Hema Singh, and R. M. Jha

Centre for Electromagnetics
CSIR-National Aerospace Laboratories, Bangalore 560017, India
hemasingh@nal.res.in, jha@nal.res.in

Abstract ― This paper presents the scattering estimation and analysis of an arbitrary phased array with parallel, centre-fed dipole elements, in the presence of mutual coupling. The total Radar Cross Section (RCS) of the uniform dipole array is computed by considering the signal reflections within the array system. The results are shown for two types of feed networks, *viz.* series feed and parallel feed. The scattering due to higher order reflections and edge effects are neglected. The analytical formulae presented for array RCS emphasize the dependence of scattered field on the design parameters, like dipole length, inter-element spacing, geometrical and electrical properties of phase shifters, couplers and terminal impedances. The results indicate that the mutual coupling effect on the overall RCS pattern is identical for both equal and unequal length dipole arrays. This paper identifies the design parameters that can be optimized towards the RCS control of phased array. These parameters include dipole-length, geometric configuration and terminal impedance.

Index Terms ― Dipole array, feed network, impedance mismatch, Radar Cross Section (RCS), reflection, transmission.

I. INTRODUCTION

Radar Cross Section (RCS) relates the electromagnetic energy at the receiver due to the reflection from the target to the electromagnetic energy impinging on it. The total antenna radar cross section consists of both structural RCS and antenna mode RCS [1]. However, for an antenna array operating within the frequency band similar to that of radar, the scattering due to antenna mode becomes predominant [2]. An efficient antenna system is required to meet the requirements of both optimum radiation characteristics and low detectability. In few cases, the antenna RCS becomes even greater than the structural RCS of the platform. Hence, it is essential that RCS of an object is reduced without affecting its radiation performance [3]. In order to achieve this objective, a detailed and accurate analysis of antenna mode scattering is required.

The estimation of antenna array scattering should include the effect of feed network architecture, terminating impedance, and mutual coupling. The total scattered field of an antenna array comprises of the fields reflected from different impedance mismatches at each level of feed network [4]. The corresponding scattered field magnitudes can be expressed in terms of reflection coefficients and terminal impedances of the array elements. Further, the values of the terminal impedances are influenced by the mutual coupling effect, which depends on the array geometry. This makes it crucial to analyze the signal path through each of the junction and mismatches within the antenna system towards the RCS estimation of phased array.

The scattering behavior of phased array has been determined and analyzed using various techniques. A finite dipole array has been studied in view of its radiation and scattering characteristics with the compensation of coupling effect [5]. The moment method along with RWG basis functions is used to calculate scattered field of equal half-wavelength dipoles, in the presence of mutual coupling. Although, the parametric analysis of scattering behavior of dipole array is presented, the feed network is not considered. The

Submitted On: July 4, 2013
Accepted On: September 7, 2014

numerical technique like FDTD method is also employed to calculate the scattering from impedance loaded dipole array without feed network [6].

The scattering behavior of antenna array with feed network has been reported but for infinitesimal dipole array [2], [7]. Moreover, the results presented ignore the mutual coupling effect in between the dipole elements. However, in a practical phased array, one cannot ignore the finite dimensions of antenna elements, coupling effect and the role of feed network while estimating the antenna RCS. The RCS of finite dipole array with series and parallel feed network including mutual coupling effect has been determined in terms of network parameters [8]. The dipoles were considered to be of equal length in different geometric configurations. In this paper, the RCS estimation of arbitrary dipole array for both series and parallel feed network is presented. In particular, the array design for unequal-length dipoles differs from earlier work [8] in two aspects. At first, it uses an extra component, which can be either the waveguide bend or the transmission line, in order to connect the dipole terminals to the corresponding phase-shifter. This extra component is taken as perfectly matched line towards the phase-shifters so as to have zero contribution towards total array RCS, for the sake of convenience. Otherwise, the impedance mismatch within this extra line is to be included in the calculations. Secondly, the dipole lengths are taken to be unequal as an attempt towards the RCS reduction within the arbitrary array system.

In this paper, an arbitrary compact dipole array is considered, in which the dipole can be either equal-length or unequal-length. Unlike [9], the results include both linear and planar dipole array.

The scattered field is determined in terms of reflections and transmissions of the signal propagating through the levels of the array system. It is the impedance mismatch at each level of the feed that results in the total scattering cross section of the array system. In the subsequent sections, the detailed analytical description of the RCS estimation of dipole array is presented. The equations derived can be used for both equal and unequal-length dipole array, with either series or parallel feed network.

II. RCS OF DIPOLE ARRAY

A uniform linear array of centre-fed dipoles each with length of $2l_n$, n=1,2,…N is considered. The inter-element spacing is taken as d and the staggered height of the dipoles from the reference plane is assumed to be h_n. The geometry of dipole array considered is generalized and it can be converted to any standard array configuration, like side-by-side, collinear or parallel-in-echelon by appropriate changes in the design parameters.

The dipoles in the array are excited by a feed network comprising of extra component, phase-shifters and couplers, in order from radiators towards the receive port. Assuming the dipoles in the array to be lossless and x-polarized, the scattered field at n^{th} dipole is given as [2], [8]:

$$\left|\vec{E}_n^s(\theta,\varphi)\right| = \left\| \left[\frac{j\eta_0}{4\lambda Z_{s_n}} \left(\int_{\Delta l_n} \cos(kl_n)\, dl_n \right)^2 (\cos\theta)\, \vec{E}_n^r(\theta,\varphi) \right] \frac{e^{-j\vec{k}\vec{R}}}{R} \hat{x} \right|, \quad (1)$$

where λ is the wavelength, η_0 is the impedance of free space, $\vec{k}$ is the propagation vector, R is the distance between the target and the receiver, l_n is the length of n^{th} dipole element, $\vec{E}_n^r(\theta,\varphi)$ is the total reflected field towards the aperture, and Z_{s_n} is the impedance of n^{th} dipole element. It is pointed out that for the simpler case of isotropic source, related expression has been earlier derived by Jenn [2]. In order to determine the total RCS of N-element dipole array, scattered fields at each of its elements are summed-up. Thus, the scattered field is expressed as [8]:

$$\left|\vec{E}_n^s(\theta,\varphi)\right| = \left\| \left[\frac{j\eta_0}{4\lambda Z_{s_n}} \left(\int_{\Delta l_n} \cos(kl_n)\, dl_n \right)^2 (\cos\theta)\, \vec{E}_n^r(\theta,\varphi) \right] \frac{e^{-j\vec{k}\vec{R}}}{R} \hat{x} \right|. \quad (2)$$

The total scattered field, and hence the RCS of the dipole array can be decomposed in terms of individual reflections at each level including antenna aperture and the feed network. These reflected fields are determined by the magnitude of reflection coefficients as per the path through which the signal propagates within the array. As a result, the RCS of the dipole array is specific to the structure of the feed network used to excite the antenna elements. In this paper, the scattering from arbitrary dipole array for two different feed networks, (i) series feed and (ii) parallel feed is derived. Since the network architecture remains the same for either type of feeds till one reaches

the coupler level, the contribution to the total RCS remains identical for all the levels preceding the level of coupler(s) in antenna system.

A. Reflection at the dipole terminals

The first source of scattering for a signal impinging on the array (Fig. 1) is the junction of radiators and connectors. The corresponding RCS equation is given as:

$$\sigma_r(\theta,\varphi)=\frac{4\pi}{\lambda^2}\left|\sum_{n=1}^{N}\left\{\frac{j\eta_0}{4\lambda Z_{s_n}}\left(\int_{\Delta l_n}\cos(kl_n)\,dl_n\right)^2(\cos\theta)\,r_{r_n}e^{j2(n-1)\alpha}\right\}\right|^2, \quad (3)$$

where α is the inter-element space delay of incident wave along array axis and r_{r_n} is the reflection coefficient of n^{th} dipole, the magnitude of which is determined by the mismatch between the impedances of dipoles and the impedance of the additional line (Fig. 1) connecting the dipole terminals to the inputs of phase-shifters,

$$r_{r_n}=\left|\frac{Z_{a_n}-Z_0'}{Z_{a_n}+Z_0'}\right|. \quad (4)$$

Here, Z_0' is the impedance of the extra component (assumed to be the same as the impedance of phase-shifter Z_0) and Z_{a_n} is the impedance at the n^{th} dipole terminal, computed in the presence of coupling between the dipole elements in the array. The calculation for self and mutual impedances of a dipole array with infinitesimally thin, parallel, centre-fed, unequal length dipoles is detailed in [10] and [11], respectively.

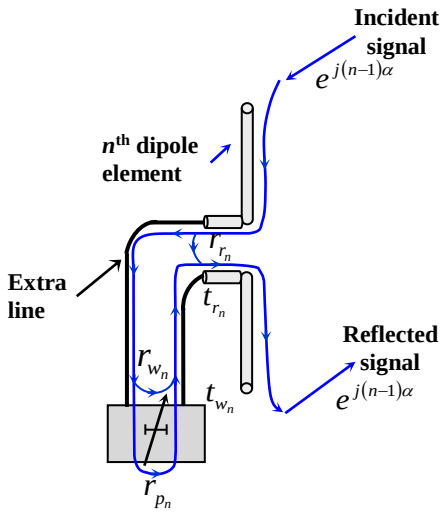

Fig. 1. The reflection and transmission coefficients till the phase-shifters.

B. Reflection at the terminals of extra component

Next, the signal would travel towards the input port of phase-shifters via the extra line. As this section of feed is assumed to be perfectly matched, its reflection coefficient will be zero. Thus, the contribution of reflections occurring at the terminals of extra line to the array RCS is:

$$\sigma_w(\theta,\phi)=0. \quad (5)$$

C. Reflection at the phase-shifters

The signal reaching the phase-shifters will get reflected at its input ports due to the impedance mismatch. The corresponding reflection coefficient r_{p_n} is given as:

$$r_{p_n}=\left|\frac{Z_{p_n}-Z_0'}{Z_{p_n}+Z_0'}\right| \ (Z_0'=Z_0 \text{ for matched extra line}), \quad (6)$$

where Z_{p_n} is the impedance at the end terminals of the delay-lines. This yields the RCS due to the reflections at the terminals of phase-shifters as:

$$\sigma_p(\theta,\varphi)=\frac{4\pi}{\lambda^2}\left|\sum_{n=1}^{N}\left\{\frac{j\eta_0}{4\lambda Z_{s_n}}\left(\int_{\Delta l_n}\cos(kl_n)\,dl_n\right)^2\times\right.\right.$$
$$\left.\left.(\cos\theta)\,t_{r_n}^2t_{w_n}^2r_{p_n}e^{j2(n-1)\alpha}\right\}\right|^2, \quad (7)$$

r_{p_n} is the reflection coefficient of n^{th} phase-shifter and t_{w_n} is the transmission coefficient of n^{th} extra line. For the matched extra line, it is always one; i.e.:

$$t_{w_n}=\sqrt{1-r_{w_n}^2}, \qquad \because r_{w_n}=0. \quad (8)$$

D. Reflection at the coupler ports

Next level in the feed network that contributes to the RCS is the junction of phase-shifters and the input ports of couplers.

***Signal reflection at the input port(s) of the couplers connected to phase-shifters*:**

The contribution of reflections at the input terminal of couplers connected to phase-shifters for the RCS of dipole array is given as:

$$\sigma_c(\theta,\varphi)=\frac{4\pi}{\lambda^2}\left|\sum_{n=1}^{N}\left\{\frac{j\eta_0}{4\lambda Z_{s_n}}\left(\int_{\Delta l_n}\cos(kl_n)\,dl_n\right)^2\times\right.\right.$$
$$\left.\left.(\cos\theta)\,t_{r_n}^2t_{w_n}^2t_{p_n}^2r_{c_n}e^{j2(n-1)\zeta}\right\}\right|^2, \quad (9)$$

where t_{p_n} is the transmission coefficient of n^{th} phase-shifter, r_{c_n} is the reflection coefficient of coupler port connected to the end of phase-shifter

[8] and $\zeta=\alpha+\alpha_s$; α_s is the inter-element phase to scan beam along the array axis. However, the calculations of the coefficients at this level depend on the type of feed. This is because, the couplers in parallel feed interact with multiple antenna elements, unlike in series feed [11].

Signal reflection at other coupler ports

The signal that enters through the input port of coupler, gets reflected within the coupler. Since the geometrical arrangement and the nature of couplers differ for the series and parallel feed network, the RCS formulation also varies.

For series feed network: Fig. 2 illustrates the signal paths and the corresponding reflected fields at n^{th} dipole in a series-fed dipole array.

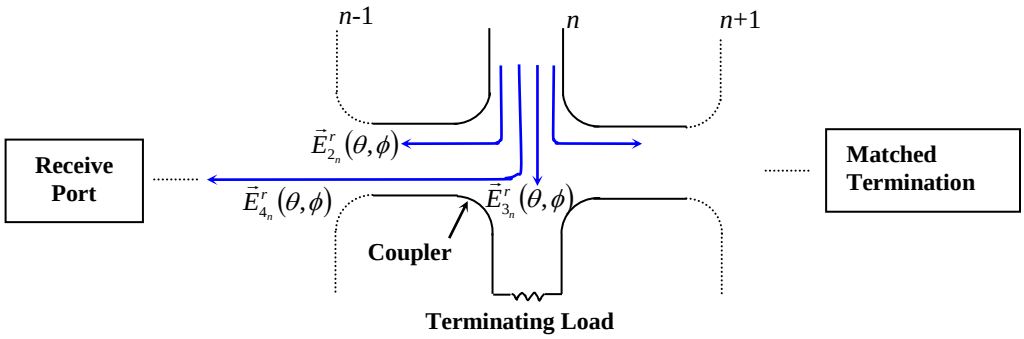

Fig. 2. Signal paths and the corresponding reflected fields at n^{th} dipole element.

The RCS due to the couplers in series feed network is expressed as:

$$\sigma_s(\theta,\varphi)=\frac{4\pi}{\lambda^2}\left|\sum_{n=1}^{N}\left[\begin{array}{l}\dfrac{j\eta_0}{4\lambda Z_{s_n}}\left(\int_{\Delta l_n}\cos(kl_n)dl_n\right)^2\times\\ (\cos\theta)\left\{\begin{array}{l}\vec{E}^r_{1_n}(\theta,\varphi)+\vec{E}^r_{2_n}(\theta,\varphi)\\ +\vec{E}^r_{3_n}(\theta,\varphi)+\vec{E}^r_{4_n}(\theta,\varphi)\end{array}\right\}\end{array}\right]\right|^2 \quad (10)$$

where $\vec{E}^r_{1_n}(\theta,\varphi)$ is the reflected field at n^{th} dipole arising from the signal propagating towards the next antenna element, given by:

$$\vec{E}^r_{1_n}(\theta,\varphi)=\left[\begin{array}{l}t_{r_n}t_{w_n}t_{p_n}r_{l_n}jc_n e^{j(n-1)\zeta}\times\\ \sum_{m=n+1}^{N}\left(t_{r_m}t_{w_m}t_{p_m}jc_m e^{j(m-1)\zeta}\prod_{i=n}^{m-1}t_{c_i}e^{j\psi}\right)\end{array}\right]. \quad (11)$$

$\vec{E}^r_{2_n}(\theta,\varphi)$ is the reflected field at n^{th} dipole arising from the signal propagating towards previous antenna element(s) in the array, given by:

$$\vec{E}^r_{2_n}(\theta,\varphi)=\left[\begin{array}{l}t_{r_n}t_{w_n}t_{p_n}jc_n e^{j(n-1)\zeta}\times\\ \sum_{m=1}^{n-1}t_{r_m}t_{w_m}t_{p_m}r_{l_m}jc_m e^{j(m-1)\zeta}\prod_{i=m}^{n-1}t_{c_i}e^{j\psi}\end{array}\right]. \quad (12)$$

$\vec{E}^r_{3_n}(\theta,\varphi)$ is the reflected field at n^{th} dipole due to signal propagating towards the terminating load, given by:

$$\vec{E}^r_{3_n}(\theta,\varphi)=r_{l_n}t^2_{r_n}t^2_{w_n}t^2_{p_n}t^2_{c_n}e^{j2(n-1)\zeta}, \quad (13)$$

and $\vec{E}^r_{4_n}(\theta,\varphi)$ is the reflected field at n^{th} dipole due to the signal propagating towards the receive port, given by:

$$\vec{E}^r_{4_n}(\theta,\varphi)=\left[r_{in}t^2_{t_n}t^2_{w_n}t^2_{p_n}(jc_n)^2e^{j2(n-1)\zeta}\left(\prod_{i=1}^{n-1}t_{c_i}e^{j\psi}\right)^2\right]. \quad (14)$$

It can be noted that the mutual impedance is included in the calculation of coefficients (c, t_c, t_s) of the coupler level in the feed network.

For parallel feed network: The RCS due to the first level of coupler is expressed as:

$$\sigma_{sd_1}(\theta,\varphi)=\frac{4\pi}{\lambda^2}\left|\sum_{n=1,3..}^{N-1}\left\{\begin{array}{l}\dfrac{j\eta_0}{4\lambda Z_{s_n}}\left(\int_{\Delta l_n}\cos(kl_n)dl_n\right)^2\times\\ (\cos\theta)\vec{E}^r_{n_1}(\theta,\varphi)+\dfrac{j\eta_0}{4\lambda Z_{s_{(n+1)}}}\times\\ \left(\int_{\Delta l_{(n+1)}}\cos(kl_{(n+1)})dl_{(n+1)}\right)^2(\cos\theta)\vec{E}^r_{(n+1)_1}(\theta,\varphi)\end{array}\right\}\right|^2, \quad (15)$$

where

$$\vec{E}^{r}_{n_1}(\theta,\varphi)=t_{r_n}t_{w_n}t_{p_n}e^{j(n-1)\zeta}\left\{\begin{array}{l} r_{s_{1i}}c_{1i}e^{j\psi}\left(\begin{array}{l} c_{1i}e^{j\psi}t_{r_n}t_{w_n}t_{p_n}e^{j(n-1)\zeta} \\ +t_{r_{n+1}}t_{w_{n+1}}t_{p_{n+1}}e^{jn\zeta}t_{c_{1i}}\end{array}\right) \\ +r_{d_{1i}}t_{c_{1i}}\left(\begin{array}{l} t_{r_n}t_{w_n}t_{p_n}e^{j(n-1)\zeta}t_{c_{1i}} \\ +t_{r_{n+1}}t_{w_{n+1}}t_{p_{n+1}}e^{jn\zeta}c_{1i}e^{j\psi}\end{array}\right)\end{array}\right\},$$

$$\vec{E}^{r}_{(n+1)_1}(\theta,\varphi)=t_{r_{n+1}}t_{w_{n+1}}t_{p_{n+1}}e^{jn\zeta}\left\{\begin{array}{l} r_{s_{1i}}t_{c_{1i}}\left(\begin{array}{l} t_{r_n}t_{w_n}t_{p_n}e^{j(n-1)\zeta}c_{1i}e^{j\psi} \\ +t_{c_{1i}}t_{r_{n+1}}t_{w_{n+1}}t_{p_{n+1}}e^{jn\zeta}\end{array}\right) \\ +r_{d_{1i}}c_{1i}e^{j\psi}\left(\begin{array}{l} t_{r_n}t_{w_n}t_{p_n}e^{j(n-1)\zeta}t_{c_{1i}} \\ +t_{r_{n+1}}t_{w_{n+1}}t_{p_{n+1}}e^{jn\zeta}c_{1i}e^{j\psi}\end{array}\right)\end{array}\right\},$$

and the RCS due to the first level coupler is:

$$\sigma_{sd_2}(\theta,\varphi)=\frac{4\pi}{\lambda^2}\left|\sum_{n=1,5\ldots}^{N-3}\left\{\begin{array}{l} \frac{j\eta_0}{4\lambda Z_{s_n}}\left(\int_{\Delta l_n}\cos(kl_n)dl_n\right)^2(\cos\theta)\times \\ \vec{E}^{r}_{n_2}(\theta,\varphi)+\frac{j\eta_0}{4\lambda Z_{s_{(n+1)}}}\left(\int_{\Delta l_{(n+1)}}\cos\left(kl_{(n+1)}\right)dl_{(n+1)}\right)^2\times \\ (\cos\theta)\vec{E}^{r}_{(n+1)_2}(\theta,\varphi)+\frac{j\eta_0}{4\lambda Z_{s_{(n+2)}}}\times \\ \left(\int_{\Delta l_{(n+2)}}\cos\left(kl_{(n+2)}\right)dl_{(n+2)}\right)^2(\cos\theta)\vec{E}^{r}_{(n+2)_2}(\theta,\varphi) \\ +\frac{j\eta_0}{4\lambda Z_{s_{(n+3)}}}\left(\int_{\Delta l_{(n+3)}}\cos\left(kl_{(n+3)}\right)dl_{(n+3)}\right)^2\times \\ (\cos\theta)\vec{E}^{r}_{(n+3)_2}(\theta,\varphi)\end{array}\right\}\right|^2, \quad (16)$$

where, the reflected fields are expressed as

$$\vec{E}^{r}_{n_2}(\theta,\varphi)=t_{r_n}t_{w_n}t_{p_n}e^{j(n-1)\zeta}c_{1i}e^{j\psi}t_{s_{1i}}\times$$

$$\left[\begin{array}{l} r_{s_{2i'}}c_{2i'}e^{j\psi}\left\{\begin{array}{l} t_{r_n}t_{w_n}t_{p_n}e^{j(n-1)\zeta}c_{1i}e^{j\psi}t_{s_{1i}}c_{2i'}e^{j\psi}+t_{r_{n+1}}t_{w_{n+1}}t_{p_{n+1}} \\ e^{jn\zeta}t_{c_{1i}}t_{s_{1i}}c_{2i'}e^{j\psi}+t_{r_{n+2}}t_{w_{n+2}}t_{p_{n+2}}e^{j(n+1)\zeta}c_{1(i+1)}e^{j\psi} \\ t_{s_{1(i+1)}}t_{c_{2i'}}+t_{r_{n+3}}t_{w_{n+3}}t_{p_{n+3}}e^{j(n+2)\zeta}t_{c_{1(i+1)}}t_{s_{1(i+1)}}t_{c_{2i'}}\end{array}\right\} \\ +r_{d_{2i'}}t_{c_{2i'}}\left\{\begin{array}{l} t_{r_n}t_{w_n}t_{p_n}e^{j(n-1)\zeta}c_{1i}e^{j\psi}t_{s_{1i}}t_{c_{2i'}}+t_{r_{n+1}}t_{w_{n+1}}t_{p_{n+1}}e^{jn\zeta}t_{c_{1i}} \\ t_{s_{1i}}t_{c_{2i'}}+t_{r_{n+2}}t_{w_{n+2}}t_{p_{n+2}}e^{j(n+1)\zeta}c_{1(i+1)}e^{j\psi}t_{s_{1(i+1)}}c_{2i'}e^{j\psi} \\ +t_{r_{n+3}}t_{w_{n+3}}t_{p_{n+3}}e^{j(n+2)\zeta}t_{c_{1(i+1)}}t_{s_{1(i+1)}}c_{2i'}e^{j\psi}\end{array}\right\}\end{array}\right], \quad (17a)$$

$$\vec{E}^{r}_{(n+1)_2}(\theta,\varphi)=t_{r_{n+1}}t_{w_{n+1}}t_{p_{n+1}}e^{jn\zeta}t_{c_{1i}}t_{s_{1i}}\times$$

$$\left[r_{s_{2i'}}c_{2i'}e^{j\psi}\left\{\begin{array}{l} t_{r_n}t_{w_n}t_{p_n}e^{j(n-1)\zeta}c_{1i}e^{j\psi}t_{s_{1i}}c_{2i'}e^{j\psi}+ \\ t_{r_{n+1}}t_{w_{n+1}}t_{p_{n+1}}e^{jn\zeta}t_{c_{1i}}t_{s_{1i}}c_{2i'}e^{j\psi}+ \\ t_{r_{n+2}}t_{w_{n+2}}t_{p_{n+2}}e^{j(n+1)\zeta}c_{1(i+1)}e^{j\psi}t_{s_{1(i+1)}} \\ \times t_{c_{2i'}}+t_{r_{n+3}}t_{w_{n+3}}t_{p_{n+3}}e^{j(n+2)\zeta}t_{c_{1(i+1)}}t_{s_{1(i+1)}}t_{c_{2i'}}\end{array}\right\}\right.$$

$$\left.+r_{d_{2i'}}t_{c_{2i'}}\left\{\begin{array}{l} t_{r_n}t_{w_n}t_{p_n}e^{j(n-1)\zeta}c_{1i}e^{j\psi}t_{s_{1i}}t_{c_{2i'}} \\ +t_{r_{n+1}}t_{w_{n+1}}t_{p_{n+1}}e^{jn\zeta}t_{c_{1i}}t_{s_{1i}}t_{c_{2i'}}+ \\ t_{r_{n+2}}t_{w_{n+2}}t_{p_{n+2}}e^{j(n+1)\zeta}c_{1(i+1)}e^{j\psi}t_{s_{1(i+1)}}c_{2i'}e^{j\psi} \\ +t_{r_{n+3}}t_{w_{n+3}}t_{p_{n+3}}e^{j(n+2)\zeta}t_{c_{1(i+1)}}t_{s_{1(i+1)}}c_{2i'}e^{j\psi}\end{array}\right\}\right], \quad (17b)$$

$$\vec{E}^{r}_{(n+2)_2}(\theta,\varphi)=t_{r_{n+2}}t_{w_{n+2}}t_{p_{n+2}}e^{j(n+1)\zeta}c_{1(i+1)}e^{j\psi}t_{s_{1(i+1)}}\times$$

$$\left[\begin{array}{l} r_{s_{2i'}}t_{c_{2i'}}\left\{\begin{array}{l} t_{r_n}t_{w_n}t_{p_n}e^{j(n-1)\zeta}c_{1i}e^{j\psi}t_{s_{1i}}c_{2i'}e^{j\psi}+t_{r_{n+1}}t_{w_{n+1}} \\ \times t_{p_{n+1}}e^{jn\zeta}t_{c_{1i}}t_{s_{1i}}c_{2i'}e^{j\psi}+t_{r_{n+2}}t_{w_{n+2}}t_{p_{n+2}}e^{j(n+1)\zeta} \\ \times e^{j\psi}c_{1(i+1)}t_{s_{1(i+1)}}t_{c_{2i'}}+t_{r_{n+3}}t_{w_{n+3}}t_{p_{n+3}}e^{j(n+2)\zeta} \\ \times t_{c_{1(i+1)}}t_{s_{1(i+1)}}t_{c_{2i'}}\end{array}\right\} \\ +r_{d_{2i'}}c_{2i'}e^{j\psi}\left\{\begin{array}{l} t_{r_n}t_{w_n}t_{p_n}e^{j(n-1)\zeta}c_{1i}e^{j\psi}t_{s_{1i}}t_{c_{2i'}}+t_{r_{n+1}}t_{w_{n+1}} \\ \times t_{p_{n+1}}e^{jn\zeta}t_{c_{1i}}t_{s_{1i}}c_{2i'}e^{j\psi}+t_{r_{n+2}}t_{w_{n+2}}t_{p_{n+2}}e^{j(n+1)\zeta} \\ \times e^{j\psi}c_{1(i+1)}t_{s_{1(i+1)}}c_{2i'}e^{j\psi}+t_{r_{n+3}}t_{p_{n+3}}e^{j(n+2)\zeta} \\ \times t_{c_{1(i+1)}}t_{s_{1(i+1)}}c_{2i'}e^{j\psi}\end{array}\right\}\end{array}\right], \quad (17c)$$

$$\vec{E}^{r}_{(n+3)_2}(\theta,\varphi)=t_{r_{n+3}}t_{w_{n+3}}t_{p_{n+3}}e^{j(n+2)\zeta}t_{c_{1(i+1)}}t_{s_{1(i+1)}}\times$$

$$\left[\begin{array}{l} r_{s_{2i'}}t_{c_{2i'}}\left\{\begin{array}{l} t_{r_n}t_{w_n}t_{p_n}e^{j(n-1)\zeta}c_{1i}e^{j\psi}t_{s_{1i}}c_{2i'}e^{j\psi}+t_{r_{n+1}}t_{w_{n+1}} \\ \times t_{p_{n+1}}e^{jn\zeta}t_{c_{1i}}t_{s_{1i}}c_{2i'}e^{j\psi}+t_{r_{n+2}}t_{w_{n+2}}t_{p_{n+2}} \\ \times e^{j(n+1)\zeta}c_{1(i+1)}e^{j\psi}t_{s_{1(i+1)}}t_{c_{2i'}}+t_{r_{n+3}}t_{w_{n+3}}t_{p_{n+3}}\times \\ e^{j(n+2)\zeta}t_{c_{1(i+1)}}t_{s_{1(i+1)}}t_{c_{2i'}}\end{array}\right\} \\ +r_{d_{2i'}}c_{2i'}e^{j\psi}\left\{\begin{array}{l} t_{r_n}t_{w_n}t_{p_n}e^{j(n-1)\zeta}c_{1i}e^{j\psi}t_{s_{1i}}t_{c_{2i'}}+t_{r_{n+1}}t_{w_{n+1}} \\ \times t_{p_{n+1}}e^{jn\zeta}t_{c_{1i}}t_{s_{1i}}t_{c_{2i'}}+t_{r_{n+2}}t_{w_{n+2}}t_{p_{n+2}}e^{j(n+1)\zeta} \\ \times c_{1(i+1)}e^{j\psi}t_{s_{1(i+1)}}c_{2i'}e^{j\psi}+t_{r_{n+3}}t_{w_{n+3}}t_{p_{n+3}} \\ \times e^{j(n+2)\zeta}t_{c_{1(i+1)}}t_{s_{1(i+1)}}c_{2i'}e^{j\psi}\end{array}\right\}\end{array}\right]. \quad (17d)$$

The total RCS of unequal length dipole array with mutual coupling effect for series feed is given by:

$$\sigma(\theta,\varphi)=\sigma_r(\theta,\varphi)+\sigma_p(\theta,\varphi)+\sigma_c(\theta,\varphi)+\sigma_s(\theta,\varphi), \quad (18)$$

and for parallel feed network till q level of couplers, the RCS of dipole array is expressed as:

$$\sigma(\theta,\varphi)=\sigma_r(\theta,\varphi)+\sigma_p(\theta,\varphi)+\sigma_c(\theta,\varphi)+\sum_{i=1}^{q}\sigma_{sd_i}(\theta,\varphi). \quad (19)$$

III. RESULTS AND DISCUSSION

The RCS estimation of uniform linear dipole array includes mutual coupling effect. Multiple

reflections and edge effects are ignored. It is assumed that the extra component, connecting antenna element with the phase shifter in the feed network is perfectly matched.

A. RCS estimation of series-fed dipole array

First, the RCS patterns of equal and unequal length dipole arrays are compared. Two 30-element arrays of equal length $\lambda/3$ and $\lambda/4$ dipoles are considered. The $\lambda/4$ and $\lambda/3$ length dipoles are arranged alternately, so as to form an unequal length dipole array.

In all cases, the staggered height of the dipoles is taken as $\lambda/3$ below and above the reference plane for odd and even-positioned dipoles, respectively. Other design parameters are taken as d=0.25λ, Z_0=100Ω, Z_l=200Ω. The elements are excited as per Taylor amplitude distribution (-45 dB SLL; $\bar{n}$ =4). Figure 3 shows that the level of RCS is minimum for $\lambda/4$ equal-length dipole array and maximum for $\lambda/3$ equal-length dipole array. On the other hand, the RCS level of unequal length dipole array lies in between the levels of two equal-length dipole array, for major portion of the pattern. However, the RCS level of unequal length dipole array is observed to increase drastically for the aspect angles beyond ±50°. It can be inferred that the optimization of dipole lengths could facilitate the reduction and control of the array RCS.

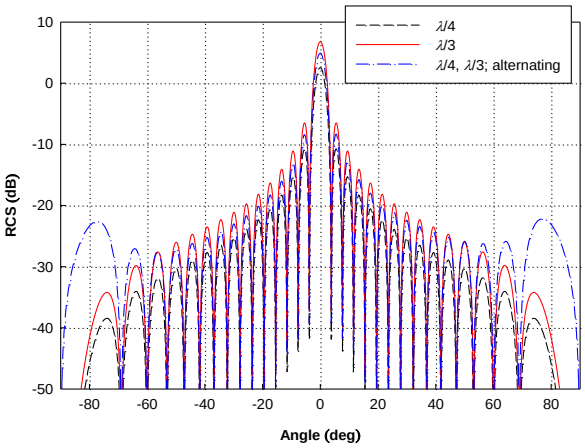

Fig. 3. Broadside RCS of equal and unequal length series-fed dipole array.

Next, the effect of mutual coupling on the scanned array RCS is demonstrated. An array of 20 thin-wire (radius=10^{-5} λ) dipoles with alternative length of $\lambda/2$ and $\lambda/3$ is considered. The staggered height of dipoles *w.r.t.* reference plane is taken as -$\lambda/4$ for odd-positioned elements and $\lambda/6$ for even-positioned elements. Other parameters are d=0.2λ, Z_0=100Ω, Z_l=40Ω; with cosine squared on pedestal element excitation. Figure 4 compares the scanned (θ_s=50°) RCS pattern of this array with and without mutual coupling effect. It can be observed that the scanned RCS of dipole array differ significantly for with and without mutual coupling cases. The variation in the scanned RCS pattern further increases for larger values of scan angle. This may be due to the inter-element interactions that vary the terminal impedances of the dipole elements, and hence the reflections within the array system and the RCS.

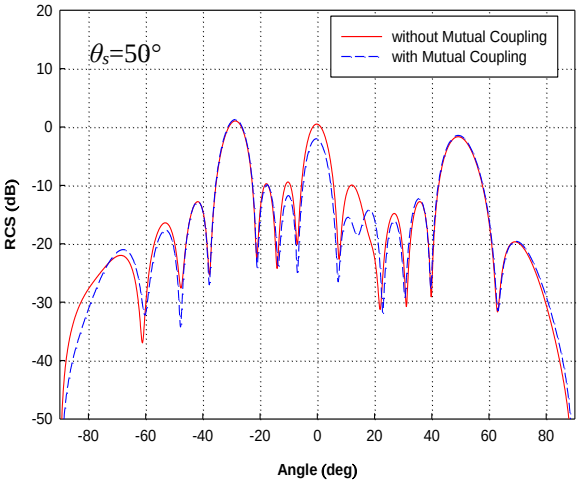

Fig. 4. Scanned (θ_s=50°) RCS patterns of 20-element unequal length linear dipole array, with and without mutual coupling effect.

Next, the effect of varying the terminal impedances of the coupler ports on the RCS pattern of 25-element unequal length uniform (d=0.2λ) dipole array is analyzed. The dipoles in the array are taken to be of lengths $\lambda/3$ and $\lambda/2$ at odd- and even-positions of the array, respectively. The staggered heights of the elements *w.r.t.* reference plane are taken to be $\lambda/4$ and -$\lambda/3$ alternatively. The amplitude distribution is Dolph-Chebyshev with -40 dB Sidelobe Level (SLL). The characteristic impedance is 75 Ω. Figure 5 shows the broadside RCS pattern for the array when the terminating impedance is varied from 0 Ω to 200 Ω.

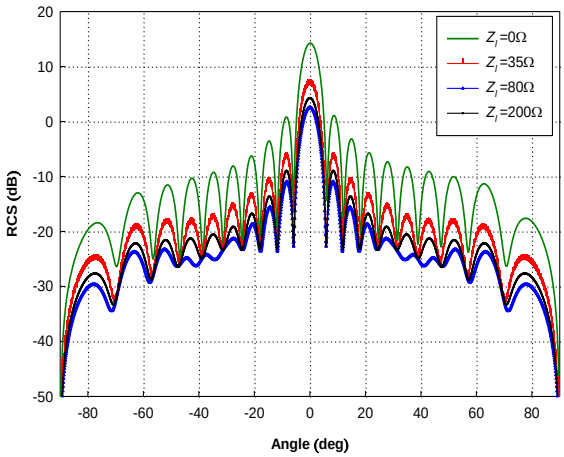

Fig. 5. Dependence of RCS pattern of a 25-element unequal-length dipole array on the terminal impedance.

It is seen that the RCS levels decrease as the terminal impedance value increases from 0 Ω to 35 Ω and further to 80 Ω. However, for terminal impedance of 200 Ω, the RCS level shows rise. This indicates that the decrease in RCS with variation of impedance terminating the coupler ports possess a limit. On reaching the limiting value of terminating impedance, the RCS level starts increasing with the load impedance Z_l. This effect is similar to the case of equal length array. This feature of terminating load dependence can be exploited for array RCS control.

B. RCS estimation of parallel-fed dipole array

The RCS of two parallel-fed linear dipole arrays, each with 32-element equal and unequal-length dipoles is computed. The dipole lengths are taken as $\lambda/2$, for equal-length array, whereas, random for unequal-length dipole array. The dipoles at odd and even positions in the array are arranged at heights of $\lambda/4$ below and above the reference line, respectively. The RCS patterns of these dipole arrays including mutual coupling effect are compared in Fig. 6. The dipoles are spaced 0.4λ apart and are excited by uniform unit amplitude distribution.

The characteristic impedance and load impedance are taken as 75 Ω and 20 Ω, respectively. Scattering is considered till second level of couplers. It is apparent that the RCS pattern of $\lambda/2$ dipole array has definite lobes *viz.* specular lobe (θ=0°), lobes due to first level coupler mismatches (θ=±38°) and lobes due to the mismatches at second level of couplers (θ=±17°). However, for the random length dipole array considered, it is difficult to identify any other lobe, except for the specular lobe. Moreover, the RCS level in case of random dipoles is observed to be less than that for $\lambda/2$ array. Although, at other aspect angles, the level of scattering in the random-length array exceeds that of equal-length array, the level is well below 0 dB, and hence less significant.

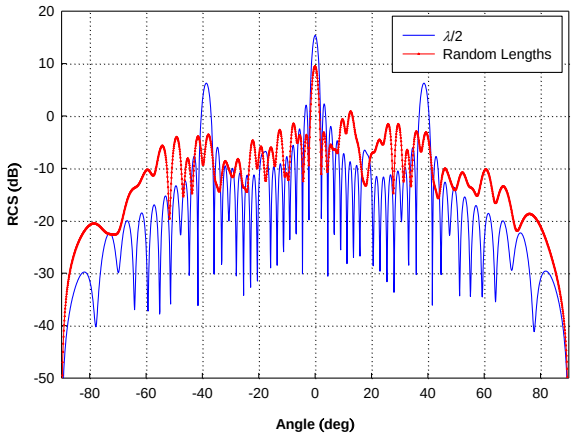

Fig. 6. Comparison of broadside RCS pattern of equal and random length dipole arrays.

Next, the mutual coupling effect in unequal-length parallel-fed dipole array is discussed. The dipole array consists of 16-elements with odd-positioned dipole lengths ($=\lambda/3+(n-1)\times0.01\lambda/3$). The dipole lengths at the even-positions decrement in the steps of $0.01\lambda/2$, starting from $\lambda/2$. All the dipoles are at the height of $\lambda/4$ above the reference plane. The inter-element spacing is taken as 0.4λ. The characteristic and load impedances are 75 Ω and 200 Ω, respectively. Figure 7 shows the broadside RCS pattern obtained, for with and without mutual coupling cases. The scattering till first level of couplers is considered. In order to analyze the effect of terminating impedance on the array RCS, a 64-element array is considered, in which the dipoles of lengths $\lambda/3$ and $\lambda/2$ are arranged alternately with staggered heights of $\lambda/4$ below and above the reference plane, respectively. The spacing between elements is 0.4λ. The influence of impedance terminating the coupler ports on the RCS pattern of such an unequal length parallel-in-echelon dipole array is shown in Fig. 8.

Dipoles are excited by uniform distribution and the characteristic impedance is taken as 75 Ω.

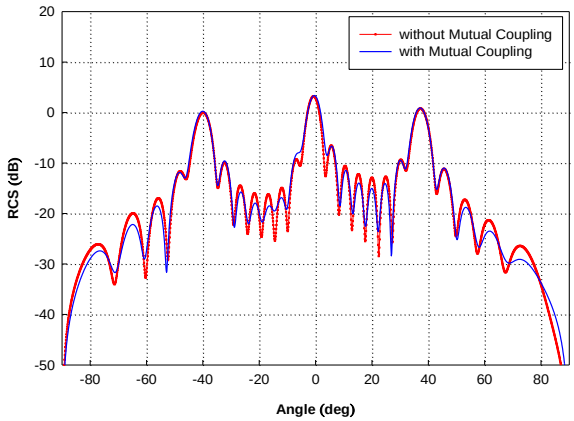

Fig. 7. Broadside RCS pattern of 16-element unequal length parallel-fed dipole array.

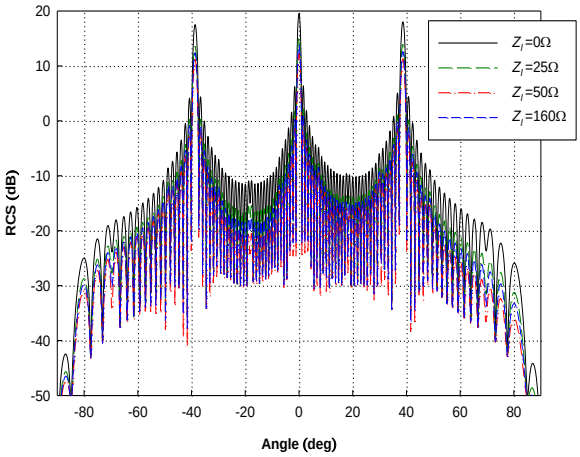

Fig. 8. Effect of varying the terminating impedances on the RCS pattern of 64-element unequal length parallel-in-echelon dipole array.

The scattering effect is considered till second level of couplers. It is observed that the RCS level is maximum for 0 Ω termination and decreases as the impedance is increased to 25 Ω and 50 Ω. However, for 160 Ω termination, the level of RCS lobes increases. This emphasizes that the concept of limiting impedance holds good, irrespective of the design parameters including length of dipoles, scan angle, amplitude distribution and the feed.

IV. CONCLUSION

This paper presents an analytical estimation of the RCS of arbitrary linear dipole array with uniform spacing. The formulation holds good for both unequal and equal length dipole arrays arranged in any random configuration. The reflections within the antenna system and the effects of mutual coupling between array elements are taken into account. The scattering due to higher order reflections is neglected and the computations are restricted till second level of couplers. The variation in the dipole lengths is shown to affect the RCS pattern of the array significantly. The dipole length could be a potential parameter for the reduction of array RCS. Moreover, the mutual coupling affects the RCS pattern for both types of feeds. The variation in RCS pattern becomes further noticeable as the scan angle of array increases, irrespective of any other design criteria. The terminating impedance is another important parameter that can be exploited for RCS control. There is a limiting value of terminating impedance beyond which RCS value of phased array increases. In broad sense, the effect of varying the design parameters on overall RCS pattern is similar in both equal- and unequal-length dipole arrays.

REFERENCES

[1] S. Hu, H. Chen, C. L. Law, Z. Shen, L. Zhu, W. Zhang, and W. Dou, "Backscattering cross section of ultra-wideband antennas," *IEEE Ant. & Wireless Propag. Letters*, vol. 6, pp. 70-73, 2007.

[2] D. C. Jenn and S. Lee, "In-band scattering from arrays with series feed networks," *IEEE Trans. Ant. & Propag.*, vol. 43, pp. 867-873, August 1995.

[3] J. Ling, S. X. Gong, B. Lu, H. W. Yuan, W. T. Wang, and S. Liu, "A microstrip printed dipole antenna with UC-EBG ground for RCS reduction," *JEWA*, vol. 23, pp. 607-616, 2009.

[4] Y. Liu and L. You, "Research on the estimation and reduction measures of antenna mode RCS of airborne phased array," *Proc. IEEE 4th Intl. Symp. on Microwave, Ant. Propag. and EMC Tech. for Wireless Comm.*, China, pp. 79-82, November 2011.

[5] Y. Liao, S. Yang, H. Ma, and Y. Hou, "Research on scattering property of finite dipole array," *Proc. of 6th Int. Conf. ITS Telecomm.*, Chengdu, China, pp. 412-415, June 2006.

[6] L. Zengrui, W. Junhong, L. Limei, and Z. Xueqin, "Study on the scattering property of the impedance terminated dipole array with finite reflector by FDTD method," *IEEE Int. Sym. on Microwave, Ant. Propag. and EMC Tech. for Wireless Comm.*, China, pp. 1003-1007, August 16-17, 2007.

[7] D. C. Jenn and V. Flokas, "In-band scattering from arrays with parallel feed networks," *IEEE Trans. Ant. & Propag*., vol. 44, pp. 172-178, February 1996.
[8] H. L. Sneha, H. Singh, and R. M. Jha, "Mutual coupling effects for radar cross section (RCS) of a series-fed dipole antenna array," *Int. J. Ant. & Propag*., vol. 2012, p. 20, August 2012.
[9] H. L. Sneha, H. Singh, and R. M. Jha, "Scattering analysis of an unequal-length dipole array in the presence of mutual coupling," *IEEE Ant. and Propag. Mag*., vol. 55, pp. 333-351, August 2013.
[10] C. A. Balanis, "Antenna theory, analysis and design," *New Jersey: John Wiley & Sons*, ISBN: 0-471-66782-X, p. 1117, 2005.
[11] H. E. King, "Mutual impedance of unequal-length antennas in echelon," *IRE Trans. Ant. & Propag*., vol. 5, pp. 306-313, July 1957.

H. L. Sneha obtained her B.E. (ECE) in 2010 from Visvesvaraya Technological University, (Belgaum), Karnataka. She worked as a NALTech Project Engineer and Project Graduate Trainee at the Centre for Electromagnetics (CEM) of CSIR-National Aerospace Laboratories, Bangalore, India. Her research interests include Radar Cross Section (RCS) of phased arrays. Sneha has co-authored twelve scientific research papers and technical reports.

Hema Singh is currently working as a Senior Scientist at the Centre for Electromagnetics of CSIR-National Aerospace Laboratories, Bangalore, India. Earlier, she was Lecturer in EEE, BITS, Pilani, India. She obtained her Ph.D. degree in Electronics Engineering from IIT-BHU, Varanasi, India. Her active areas of research are CEM for Aerospace Applications, Phased Arrays, and Radar Cross Section (RCS) Studies. Singh has co-authored one book chapter, and over 110 scientific research papers and technical reports.

Rakesh Mohan Jha is currently a Chief Scientist & Head, at the Centre for Electromagnetics, CSIR-National Aerospace Laboratories, Bangalore. Jha obtained his B.E. and M.Sc. degrees (Physics) from BITS, Pilani (Rajasthan) in 1982. He obtained his Ph.D. (Eng.) degree from the Department of Aerospace Engineering, of Indian Institute of Science, Bangalore in 1989, in the area of Computational Electromagnetics for Aerospace Applications. Jha was a SERC (UK) Visiting Post-Doctoral Research Fellow at the University of Oxford, Department of Engineering Science in 1991. He worked as an Alexander von Humboldt (AvH) Fellow at the Institute for High-Frequency Techniques and Electronics of the University of Karlsruhe, Germany (1992-1993, 1997). He was awarded Sir C.V. Raman Award for Aerospace Engineering for the Year 1999. Jha was elected Fellow of INAE (FNAE) in 2010, for his contributions to the EM Applications to Aerospace Engineering. He is also the Fellow of IETE and Distinguished Fellow of ICCES. Jha has authored or co-authored more than four hundred scientific research papers and technical reports.